The *tert*-Butyl Hydroperoxide-Induced Oxidation of Actin Cys-374 Is Coupled with Structural Changes in Distant Regions of the Protein†

Isabella DalleDonne, Aldo Milzani,* and Roberto Colombo

Department of Biology, University of Milan, via Celoria 26, I-20133 Milan, Italy

Received February 15, 1999; Revised Manuscript Received June 7, 1999

ABSTRACT: The susceptibility of monomeric actin to both methionine and cysteine oxidation when treated with the oxidizing agent *tert*-butyl hydroperoxide (t-BH) was investigated. The results show that no methionine residue was susceptible to oxidation by t-BH at concentrations of 1−20 mM, while Cys-374, one of the five cysteine residues of the actin molecule, was found to be the site of the oxidative modification. Perturbations in the intrinsic tryptophan fluorescence and the decreased susceptibility to limited proteolysis by α-chymotrypsin and subtilisin of oxidized actin give an indication of some alterations in protein conformation in subdomain 1, and in the central segment of surface loop 39−51, in subdomain 2. Urea denaturation curves indicate a lower conformational stability for the oxidized actin. G-actin structural alterations due to Cys-374 oxidation produced by t-BH result in a decrease in the maximum rate of polymerization, an increase in both the delay time and the time required for half-maximum assembly, a decrease in the elongation rate, and enhancement of the critical monomer concentration for polymerization. The results suggest that oxidation of actin Cys-374 induces structural alterations in the conformation of at least two different distant regions of the molecule. The involvement of both the C-terminus of the actin polypeptide chain and the DNase-I-binding loop in the intermonomer interactions in the polymer could account for the altered kinetics of polymerization shown by the oxidized actin.

Covalent changes caused by in vivo protein oxidation are primarily responsible for the accumulation of catalycally compromised (inactive or less active) and structurally altered enzymes during aging (*1*). Furthermore, protein oxidation may play a role in several pathological states, including inflammatory disease, atherosclerosis, neurological disorders, and cataractogenesis (*2*).

All biologically relevant oxidants—i.e., hydrogen peroxide (H_2O_2), superoxide anion (O_2^-), hydroxyl radicals, hypochlorite ions, chloramines, nitrogen oxide (NO), and peroxynitrite (formed by the fusion of NO with O_2^{*-})—are copiously produced by polymorphonuclear leukocytes (mainly by neutrophils) and other phagocitic cells on activation in defense reactions of the host. The activated cells undergo a respiratory burst during which they produce the oxidizing reagents; these are highly toxic to extracellular-invading microorganisms, tissues, as well as the neutrophils themselves, leading to the oxidation of several amino acid residues of many proteins.

Oxidative stress causes modification of cellular macromolecules and leads to cell damage (*3*−*5*). Cell rounding and plasma membrane blebbing as well as shortening of microfilaments, which aggregate side-to-side into short bundles, suggest that cytoskeletal elements of the cell cortex could represent one of the cellular targets of the biological activity of H_2O_2 (*6*−*8*), a relatively nonspecific oxidizing agent. Analysis of the cytoskeletal fraction from isolated hepatocytes treated with the thiol oxidant diamide under nonreducing conditions suggested that actin is one of the target molecules for protein thiol oxidation, as demonstrated by the formation of actin aggregates sensitive to thiol reductants (*9*). Furthermore, Omann et al. (*10*) suggested that oxidation of sulfhydryls in actin occurs in $P388D_1$ cells (a transformed murine macrophage cell line) exposed to oxidative stress. Finally, H_2O_2 alters actin dynamics in vitro (*11*, *12*).

With the exception of O_2^-, all the oxidants produced in biological systems oxidize methionine, which, together with cysteine and tryptophan, belongs to the most readily oxidized amino acid residues of proteins. The oxidation product is methionine sulfoxide, which can be reduced back to methionine by chemicals or by methionine sulfoxide reductase.

Methionine oxidation to the sulfoxide derivative can functionally have different consequences. In general, it may inactivate proteins; however, it does not necessarily cause either structural changes or loss of biological activity.

Recently, Keck (*13*) investigated the susceptibility of native recombinant interferon gamma (rlFN-gamma) and recombinant tissue-type plasminogen activator (rt-PA) to methionine oxidation induced by the alkyl hydroperoxide *tert*-butyl hydroperoxide (t-BH).[1] The results showed that two of the five methionine residues in rlFN-gamma were

† This work was supported by Grant CT-98.00428.CT04.115.19967 from the Consiglio Nazionale delle Ricerche and by MURST (Ministero della Ricerca Scientifica e Tecnologica), Rome (Italy).

* To whom correspondence should be addressed at the Department of Biology, University of Milan, via Celoria 26, I-20133 Milan, Italy. Fax: +390226604462. Phone: +390226604473. E-mail: quack@mailserver.unimi.it.

[1] Abbreviations: G-actin, monomeric actin; F-actin, filamentous (polymerized) actin; DTNB, 5,5′-dithiobis(2-nitrobenzoic acid); TNB, thionitrobenzoate; 1,4-PBM, *N*,*N*′-1,4-phenylenebismaleimide; t-BH, *tert*-butyl hydroperoxide; pyrene, *N*-(1-pyrenyl)iodoacetamide; GdmCl, guanidine hydrochloride; ANP, *N*-(4-azido-2-nitrophenyl)putrescine.

10.1021/bi990367k CCC: $18.00
Published on Web 09/03/1999

susceptible to oxidation by t-BH, while three of the five methionines in rt-PA were found to be oxidizable. The oxidized methionine residues were found to be in the sulfoxide form, and no other residue(s) appeared to be modified during t-BH treatment. Furthermore, during treatment of a native protein with t-BH, only the exposed methionine residues were oxidized stoichiometrically. Therefore, t-BH should be useful for oxidizing surface methionine residues in a protein and for identifying surface methionine residues in a protein of unknown structure. On the other hand, damage to cytoskeletal protein thiols by the formation of high molecular aggregates was caused in human red blood cells by t-BH treatment and was proposed to be related to the hemolytic process (*14*). t-BH-induced modification of protein thiols, in human red blood cells, has been confirmed by isoelectric focusing analysis (*15*).

We describe here the susceptibility of actin to methionine and cysteine oxidation when treated with t-BH and the effect it has on the structure of actin monomers as well as filament assembly.

MATERIALS AND METHODS

Reagents. Subtilisin Carlsberg (EC 3.4.21.62, from *Bacillus licheniformis*), α-chymotrypsin (EC 3.4.21.1, tosyllysinechloromethane-treated, type XIII: from bovine pancreas), ATP (disodium salt), *N*,*N*′-1,4-phenylenebismaleimide (1,4-PBM), phalloidin, and *tert*-butyl hydroperoxide (t-BH) were purchased from Sigma Chemical Co. (St. Louis, MO). Cyanogen bromide (CNBr) was purchased from Aldrich Chimica (Milan, Italy). *N*-(1-Pyrenyl)iodoacetamide was obtained from Molecular Probes (Eugene, OR). All other reagents were of analytical grade.

Preparation and Modifications of Actin. Rabbit skeletal muscle actin was prepared according to the method of Spudich and Watt (*16*) with an additional Sephadex G-150 gel filtration step. G-actin in 2 mM Tris-HCl, pH 7.5, 0.5 mM DTT, 0.2 mM ATP, 0.2 mM $CaCl_2$, 1.5 mM NaN_3 (buffer G) was lyophilized after the addition of 2 mg of sucrose/mg of actin and stored at −20 °C. To prepare G-actin, the lyophilized powder was dissolved in and dialyzed for at least 24 h against buffer G depleted of DTT and NaN_3 (buffer A). G-actin (molecular mass 42.3 kDa) concentration was determined by measuring the absorbance at 290 nm, using an extinction coefficient of 0.617 mg^{-1} mL cm^{-1} (*17*).

N-(1-Pyrenyl)iodoacetamide-labeled actin (pyrene-actin) was prepared by the method of Tellam and Frieden (*18*). The pyrene-actin concentration and the extent of labeling were determined by measuring the absorbance at 290 and 344 nm, by using $E_{344} = 2.2 \times 10^4$ M^{-1} cm^{-1} for the protein−dye complex, in agreement with Kouyama and Mihashi (*19*) and Cooper et al. (*20*).

Prior to use, G-actin solutions were clarified by a 60-min centrifugation at 100000*g*. Before sample preparation, protein solutions and buffers were filtered with 0.20 μm disposable filters and degassed. The experiments were executed in buffer A, unless stated otherwise.

tert-Butyl Hydroperoxide Treatment on Actin Monomers. G-actin (23.64 μM) was treated overnight with various concentrations of t-BH, at 25 °C. The removal of t-BH was accomplished by gel filtration on PD-10 columns (Sephadex G-25 M, Pharmacia Biotech) or by exhaustive dialysis against buffer A at 4 °C. All reported experiments have been carried on in t-BH-free media.

Chemical Cleavage at Met Residues. Oxidized actin samples (11.82 μM, 0.4 mL) were treated with 40 μL of 10% (w/v) CNBr in 70% formic acid. After 2 h at 25 °C, formic acid and excess reagent were removed by rotary evaporation. Lyophilized samples were dissolved in 0.1 M NaOH and added with 6× SDS−PAGE sample buffer for the electrophoretic run on 15% (w/v) polyacrylamide slab gels (*21*).

To unfold G-actin and expose all its methionine residues, actin monomers (23.64 μM, 1 mL) were lyophilized, dissolved in 8 M urea, and then treated overnight with various concentrations of t-BH. After exhaustive dialysis against buffer A, oxidized actin monomers were cleaved with CNBr as described above.

Ellman Assay for Cys Residues. Oxidized actin monomers (11.82 μM, 1 mL) were added with 50 μL of 3 mM 5,5′-dithiobis(2-nitrobenzoic acid) (DTNB or Ellman's reagent) which reacts with the free sulfhydryl side chain of cysteine to form an S−S bond between the protein and a thionitrobenzoate (TNB) residue. After incubation for 2 h at 25 °C, the number of cysteines was determined by measuring the absorbance of the released TNB anion.

To unfold G-actin and expose all its cysteine residues, oxidized actin monomers (11.82 μM, 1 mL) were lyophilized under vacuum and then dissolved in 6 M guanidine hydrochloride (GdmCl). After incubation for 15 min at 25 °C, the number of cysteines was determined by measuring the absorbance of the released TNB anion.

Solutions of DTNB and GdmCl were prepared in 0.1 M phosphate buffer, pH 7.3. The molar absorbance of the TNB anion is $E_{412} = 13.7$ mM^{-1} cm^{-1} in 6 M GdmCl and $E_{412} = 14.15$ mM^{-1} cm^{-1} in its absence (*22*).

Cross-Linking between Cys-374 and Lys-191 in Adjacent Subunits of Actin Filaments. Cross-linking between adjacent subunits of F-actin was performed according to Millonig et al. (*23*). Immediately before each assay, an aliquot of the 5 mM PBM stock solution in 100% dimethylformamide was diluted to twice the final cross-linker concentration with 10 mM sodium borate, pH 9.2, containing 100 mM KCl and 2 mM $MgCl_2$. Then 100 μL of the PBM-containing sodium borate solution was added to 100 μL of F-actin (actin:PBM molar ratio 1:2). Ten minutes later, the cross-linking reaction was quenched by the addition of 100 μL of 3× SDS−PAGE sample buffer containing 5% (v/v) β-mercaptoethanol. SDS−PAGE of cross-linked actin oligomers was performed according to Laemmli (*21*) on 7.5% (w/v) polyacrylamide slab gels. The gels were stained with Coomassie brilliant blue R-250. Densitometric scans of protein bands were performed with a Umax UC840 scanner.

Enzymatic Cleavage at Met-44 and Met-47 Residues. All digestions were carried out at the actin concentration of 23.64 μM, at 25 °C. Enzymes were dissolved just before use and kept in ice before digestion. α-Chymotrypsin digestion was carried out at an enzyme:protein mass ratio of 1:50 and was stopped with 2 mM PMSF. Subtilisin digestion was carried out at an enzyme:protein mass ratio of 1:1500 and was stopped with 2 mM PMSF. The samples were mixed with 6× SDS−PAGE sample buffer. Digestion products were analyzed by SDS−PAGE (*21*) on 15% (w/v) polyacrylamide slab gels, which were stained with Coomassie brilliant blue

R-250. Densitometric scans of protein bands were performed with a Umax UC840 scanner.

Since methionine oxidation of both α-chymotrypsin and subtilisin directly correlates with loss of enzymatic activity (*24*, *25*), we evaluated the possible inhibitory effect of t-BH on enzyme activity, in case trace quantities of t-BH remained in the medium after gel filtration or exhaustive dialysis. The activity of both α-chymotrypsin and subtilisin was assayed by digesting native G-actin in the presence of 1−5 mM t-BH. No differences were observed in digestion products in t-BH-containing samples compared to control. Therefore, we can rule out a loss of enzymatic activity due to possible trace amounts of t-BH in the medium.

Tryptophan Intrinsic Fluorescence of G-Actin. The tryptophan fluorescence of G-actin (11.82 μM) was obtained by excitation at 297 nm (*26*). Intensity changes in the emission fluorescence were measured at 25 °C at all wavelengths ranging between 300 and 400 nm. Fluorescence data were collected with a Kontron SFM-25 spectrofluorometer, using 10 × 10 mm quartz cuvettes.

Urea Denaturation Curves. To unfold G-actin, both native and oxidized actin monomers (4.73 μM) were treated with various concentrations of urea for 20 h at 25 °C. The tryptophan intrinsic fluorescence at 324 nm was obtained by excitation at 297 nm. Since solutions of urea slowly decompose to form cyanate and ammonium ions, which are capable of chemically modifying the amino groups of proteins, urea stock solution (10 M, in buffer A) was prepared and used within 1 day.

For analyzing denaturation curves, we assumed a two-state mechanism for the folding/unfolding reaction. This method assumes that at equilibrium only the fully folded or native protein and the fully unfolded or denatured protein are present at significant concentrations. The fraction of total protein in the unfolded conformation (f_U) was calculated using

$$f_U = (IF_F - IF)/(IF_F - IF_U)$$

where IF is the actin intrinsic fluorescence measured at 324 nm and IF_F and IF_U represent the values of the intrinsic fluorescence characteristic of the folded and unfolded protein, respectively. The values of IF_F and IF_U for any point in the transition region are obtained by extrapolation of the pre- and post-transition base lines.

Light Scattering Measurements. Actin polymerization was followed at 25 °C by the increase in the 90° light scattering at 546 nm (*27*), with excitation and emission slits set at 10 and 5 nm, respectively. The spectrofluorometer was equipped with Wind 25 software. Light scattering intensities [$R(\vartheta)$] were expressed in percentage, considering 100% the signal from a standard sample (11.82 μM G-actin polymerized by 100 mM KCl and 2 mM $MgCl_2$ at 25 °C) when no further changes in $R(\vartheta)$ were observed.

Pyrene-actin Fluorescence Measurements. G-actin polymerization was monitored by measuring the fluorescence enhancement of trace quantities of pyrene-actin (10% of 11.82 μM total actin), in a thermostated cuvette at 25 °C. The spectrofluorometer was equipped with a neutral density filter (50%), to avoid pyrene-actin photobleaching, and a cutoff filter (390 nm), to minimize the contribution of light scattering to the data. The excitation and emission wavelengths were 365 and 407 nm, respectively. Fluorescence intensities were expressed in percentage, considering 100% the signal from a standard sample (11.82 μM G-actin polymerized by 100 mM KCl and 2 mM $MgCl_2$ at 25 °C) when no further changes in fluorescence intensity were observed.

High-Shear Viscosity Measurements. High-shear viscosity was measured at 25 °C in Ostwald-type viscometers with a sample volume of 0.5 mL and a buffer flow time of 25−30 s. Results are expressed as specific viscosity (η_{sp}) in centiStokes (1 Stoke = 10^{-4} m^2 s^{-1}), which is defined as follows: $\eta_{sp} = (t_s/t_b) - 1$, where t_s is the sample flow time and t_b is the buffer flow time.

Preparation of Phalloidin-Stabilized Actin Seeds. A stock solution of phalloidin-stabilized actin seeds was prepared by polymerizing G-actin at a concentration of 24.5 μM in the absence of salt by incubation for 24 h at 25 °C with equimolar phalloidin (*28*). To use the seeds, aliquots of the stock solution were diluted 10-fold with buffer A and sonicated at 50 W for two 30-s periods with a Braun sonifier. Seed solution was then stored in ice at least 3 h before using it, thereby ensuring a negligible reannealing process.

RESULTS

Tryptophan Intrinsic Fluorescence. The fluorescence of proteins originates from phenylalanine, tyrosine, and tryptophan residues. In proteins that contain all three aromatic amino acids, fluorescence is usually dominated by the contribution of the Trp residues, because both their absorbance at the wavelength of excitation and their quantum yield of emission are considerably greater than the respective values for Tyr and Phe. Fluorescence emission is much more sensitive to changes in the environment of the chromophore than is light absorption. As the lifetime of the excited state is long, a broad range of interactions or perturbations can influence this state and thereby the emission spectrum. Fluorescence is thus an excellent spectroscopic probe to investigate conformational changes of proteins. Changes in protein conformation, such as unfolding, very often lead to large changes in fluorescence emission. In proteins that contain tryptophan, both shifts in wavelength and changes in intensity are generally observed upon unfolding. Trp emission spectra (Figure 1) reveal a remarkable reduction (approximately by 20%) of the fluorescence intensity of actin oxidized with t-BH compared to that of native G-actin. The fluorescence intensity lowering, not accompanied by the spectral red shift characterizing denatured actin, indicates that a perturbation of G-actin structure occurred during treatment with t-BH.

Urea Denaturation Curves and Conformational Stability. Since tryptophan fluorescence showed that changes in the specific three-dimensional structure of the polypeptide chain (i.e., the correctly folded structure) accompany actin oxidation induced by t-BH, we assessed whether protein stability was affected by actin oxidation.

Figure 2 illustrates the fraction of total protein in the unfolded conformation (f_U, or fractional denaturation) for both native and oxidized actin as a function of urea concentration. The mole fraction of denatured actin goes from a minimum of 0 at low urea concentrations to a maximum of 1 above a critical urea concentration. Denaturation curves allow us to determine the concentration of urea required to

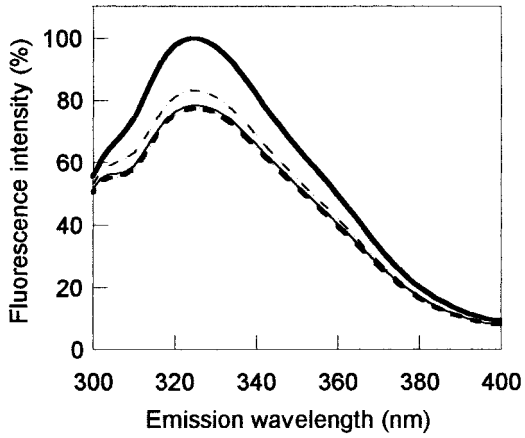

FIGURE 1: Fluorescence emission spectra of G-actin. After overnight treatment with t-BH and removal of excess oxidizing agent as described under Materials and Methods, tryptophan fluorescence emission spectra were taken at 11.82 μM G-actin with λ_{ex} set at 297 nm. G-actin treated with 1 mM (thin dashed trace), 10 mM (thick dashed trace), and 20 mM (thin solid trace) t-BH shows a reduction in the fluorescence intensity in comparison with native G-actin (thick solid trace).

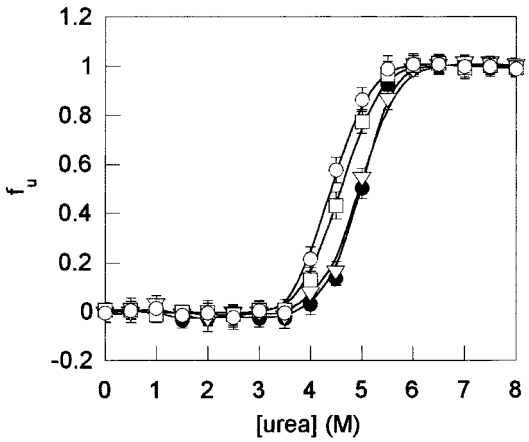

FIGURE 2: Conformational stability of actin following chemical modification by t-BH. Urea denaturation curves were constructed for native and oxidized G-actin, prepared as described in Figure 1, from measurements of the tryptophan intrinsic fluorescence at 324 nm with λ_{ex} set at 297 nm. The mole fraction of unfolded protein (f_U) as a function of urea concentration was calculated as described under Materials and Methods. Native G-actin (filled circles); G-actin treated with 1 mM (open triangles), 10 mM (open squares), and 20 mM (open circles) t-BH, respectively. Error bars represent the standard deviations of three replicate measurements.

reach 50% unfolding (or denaturation), i.e., where $f_U = 0.5$; this value is referred to as c_m (the midpoint concentration). For the data in Figure 2, c_m values are 5 M urea for control actin as well as actin oxidized with 1 mM t-BH, and 4.6 and 4.4 M urea for actin oxidized with 10 and 20 mM t-BH, respectively.

Enzymatic Cleavage by Subtilisin and α*-Chymotrypsin.* We used proteolytic susceptibility as a probe for identifying regions of the actin polypeptide chain where structural rearrangements took place as a consequence of the oxidation produced by t-BH. The time courses of cleavage by α-chymotrypsin of the peptide bond between Met-44 and Val-45 to generate a 35-kDa C-terminal fragment, which is subsequently degraded from its N-terminus to produce a 33-kDa derivative (*29*), are illustrated in Figure 3A. t-BH treatment of monomeric actin results in a decrease in the rate of decay of the actin band. The time courses of cleavage by subtilisin of the peptide bond between Met-47 and Gly-48 to produce a 35-kDa C-terminal fragment (*30*) are illustrated in Figure 3B. Oxidation of G-actin produced by increasing concentrations of t-BH results in a dose-dependent decrease in the rate of decay of the actin band.

Chemical Cleavage by Cyanogen Bromide. Since t-BH was found to be a methionine-specific oxidant (*13*), besides being a cysteine oxidant, the sensitivity of actin methionine residues to oxidation with t-BH was investigated by CNBr treatment (Figure 4). Cyanogen bromide causes cleavage of proteins at the level of their methionines, but not if Met residues are oxidized to methionine sulfoxide. Oxidation of both native and unfolded actin with 1, 10, and 20 mM t-BH produces SDS−PAGE patterns of the CNBr fragments identical with that of control actin (Figure 4A,B, central panels). This result indicates that, at the concentrations used in this work, t-BH treatment does not modify any methionine residue in the actin molecule.

At higher (0.5 M) t-BH concentration , i.e., at higher molar ratio of t-BH to methionine residues, actin oxidation results in a decreased susceptibility to CNBr-induced fragmentation (Figure 4A, right panel), indicating that t-BH oxidized one or more methionine residues, which are on the surface of the actin molecule and/or exposed to the solvent. Treatment of unfolded actin with 0.5 M t-BH leads to an almost complete failure of CNBr cleavage, indicating the conversion of almost all methionine residues to their sulfoxide derivative (Figure 4B, right panel).

Free Thiol Quantification. Rabbit muscle actin contains five cysteine residues (Cys-10, Cys-217, Cys-257, Cys-285, and Cys-374) existing in the reduced form (*31*). The most reactive thiol group of actin has been identified as the cysteine residue next to the carboxy terminus which, according to Vandekerckhove and Weber (*32*), is Cys-374 (*33*). G-actin, prepared as normally in the presence of ATP, exposes one fast-reacting thiol group, that is, Cys-374. In addition to oxidation of methionine (*13*), t-BH also oxidizes cysteine (*15*). Then, it was considered that the alteration in the actin monomer structure due to the effect of t-BH resulted from the oxidation of Cys residue(s) to cysteic acid. Accordingly, the Cys content of G-actin treated overnight with different concentrations of t-BH was determined. The number of exposed Cys residue(s) in folded actin, determined by reaction with DTNB (*34*), diminished from about 1 in native G-actin to 0.2 in G-actin oxidized with 10 and 20 mM t-BH (Figure 5). In accordance with data on the amount of Cys per actin monomer (*31*), we found 4.8 Cys residues per unfolded monomer by titration with DTNB in the presence of 6 M guanidine hydrochloride. When G-actin solutions were previously incubated with increasing concentrations of t-BH, the number of Cys per unfolded monomer progressively decreased from 4.8 to 4.0 (Figure 5). These observations indicate that oxidation of actin thiol groups produced by t-BH involves only Cys-374.

Cross-Linking between Cys-374 and Lys-191 in Adjacent Subunits of F-Actin. In filamentous actin, subunit contacts occur between subdomain 1, at Cys-374, on one actin subunit and subdomain 4, at Lys-191, on the adjacent subunit along the genetic helix of the actin filament (*23*, *35*). To confirm that t-BH oxidizes Cys-374 in actin monomer, we used the bifunctional sulfhydryl cross-linking reagent 1,4-PBM to

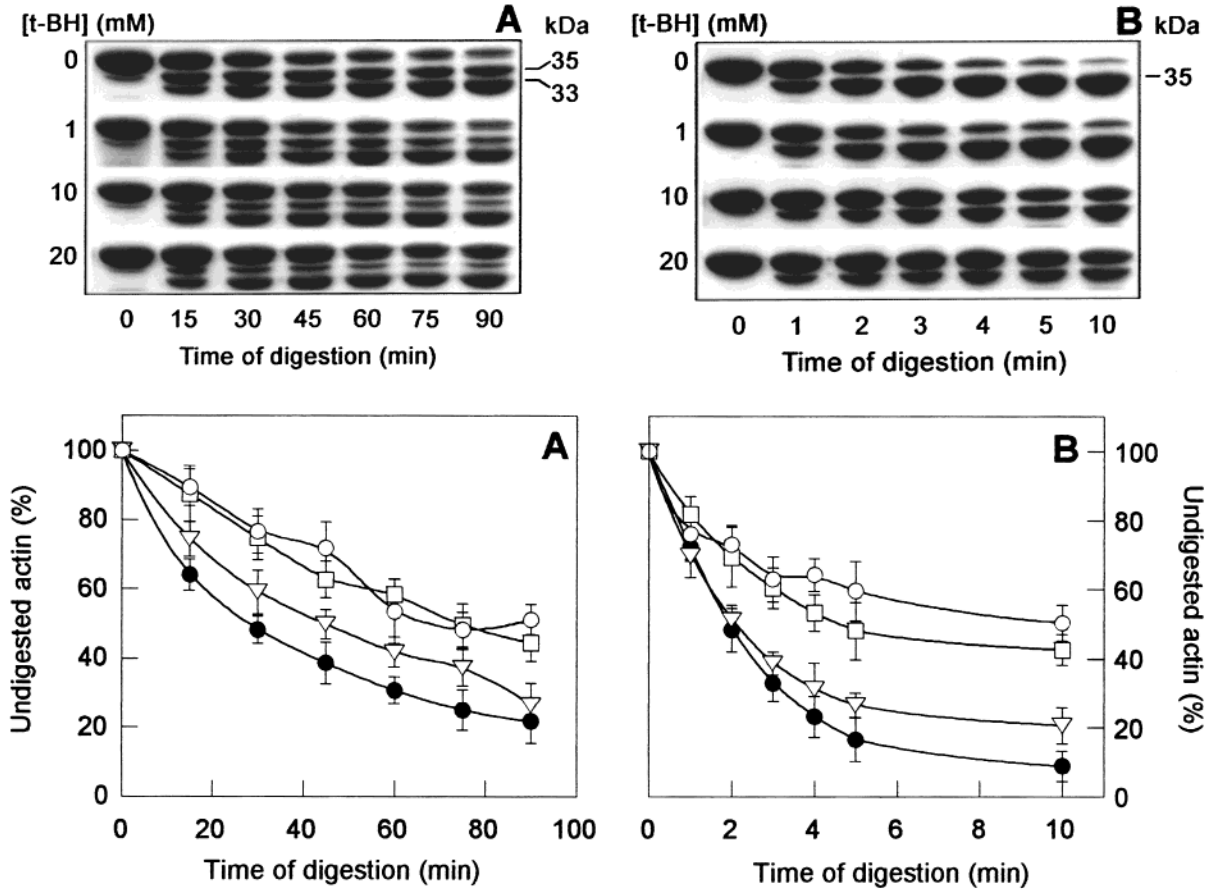

FIGURE 3: Electrophoretic patterns and time courses of decay of native and t-BH-oxidized G-actin during enzymatic digestion with α-chymotrypsin and subtilisin. Digestions of oxidized G-actin, prepared as described in Figure 1, were carried out at the actin concentration of 23.64 μM, at 25 °C. (A) α-Chymotrypsin digestion of t-BH-treated G-actin was carried out at an enzyme-to-protein mass ratio of 1:50. The upper panel shows the electrophoretic pattern of the disappearance of the intact actin band and of the appearance of main digestion products. The C-terminal 35-kDa fragment and its 33-kDa derivative are indicated. In the lower panel, the concentration of undigested actins is expressed as a percentage of the initial actin concentration. (B) Subtilisin digestion of t-BH-treated G-actin was carried out at an enzyme-to-protein mass ratio of 1:1500. The upper panel shows the electrophoretic pattern of the disappearance of the intact actin band and of the appearance of the main digestion products. The C-terminal 35-kDa fragment is indicated. In the lower panel, the concentration of undigested actins is expressed as a percentage of the initial actin concentration. In both (A) and (B): native G-actin (filled circles); G-actin treated with 1 mM (open triangles), 10 mM (open squares), and 20 mM (open circles) t-BH, respectively. Error bars represent the standard deviations of three replicate measurements.

covalent cross-link Cys-374 to Lys-191 in adjacent subunits of oxidized F-actin.

In native F-actin, the cross-linking assay yielded a 86-kDa apparent molecular mass dimer (i.e., the so-called "lower dimer", LD), a major "upper dimer" band with anomalous electrophoretic mobility corresponding to an apparent molecular mass of about 130 kDa (UD), and higher molecular mass bands (HOs, >200 kDa) that probably represent F-actin trimers and higher oligomers (*23*, *36*, *37*) (Figure 6). According to protein chemical analysis, Lys-191 of one actin subunit is cross-linked to Cys-374 of another subunit in the UD (*37*). The LD cross-link most likely occurs between Cys-374 of both subunits (*23*). The LD can migrate very similarly to a polypeptide chain of twice the molecular mass of an actin monomer by SDS−PAGE, whereas the UD cannot adopt a relaxed linear conformation and hence exhibits an anomalous mobility by SDS−PAGE. In oxidized F-actin samples, the UD concentration markedly decreases with the increase in the t-BH concentration used to oxidize actin monomers (that is, probably, with the amount of oxidized monomers in F-actin samples), whereas both LDs and HOs cannot be detected (Figure 6).

Kinetics of Actin Polymerization. Polymerization of G-actin is thought to occur as a result of partial neutralization of surface charge by cations present as neutral salts in the assembly buffer. The G-actin assembly in solution can be initiated by the addition of nucleating salts at physiological concentration (i.e., 100 mM KCl and 2 mM $MgCl_2$). The kinetics of salt-induced oxidized G-actin assembly are shown in Figure 7. Polymerization of oxidized actin monomers as followed by the increase in light scattering intensity [$R(\vartheta)$] is slower and less efficient than the corresponding polymerization of control actin (Figure 7, left panel). The maximum polymerization rate [expressed as enhancement of $R(\vartheta)$ s^{-1}] shows 29%, 52%, and 55% inhibition in the 1, 10, and 20 mM t-BH-treated actin samples, respectively. In addition, in oxidized actin samples, the plateau levels of light scattering intensity decrease in a dose-dependent fashion compared to the steady-state value of the native F-actin sample.

The retarded polymerization was also observed when it was followed by the fluorescence enhancement of trace quantities of pyrene-actin (Figure 7, right panel). In agreement with light scattering data, oxidized actin shows a decrease both in the maximum rate and in the extent of

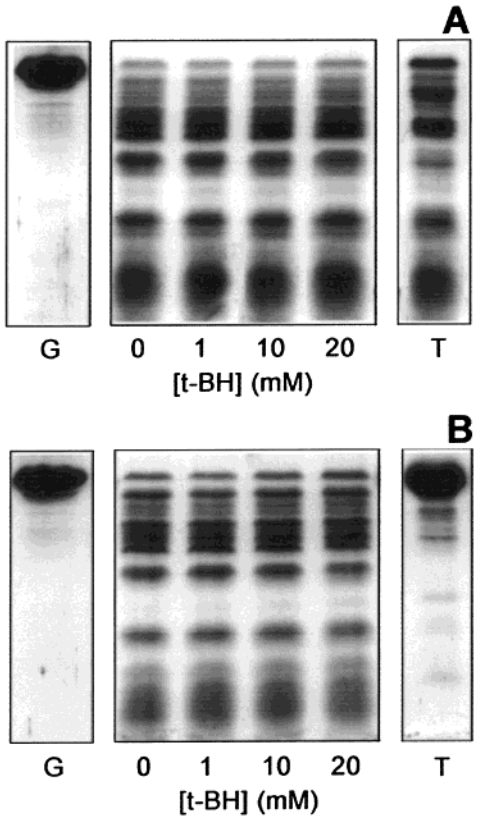

FIGURE 4: Cyanogen bromide cleavage of native and t-BH-oxidized G-actin. (A) CNBr-induced fragmentation of oxidized actin, prepared as described in Figure 1, was performed at the protein concentration of 11.82 μM with 1% (w/v) CNBr in 70% formic acid. The cleavage reaction was allowed to proceed for 2 h at 25 °C. SDS−PAGE analysis of undigested actin (G, left panel), actin treated with CNBr after oxidation with different concentrations of t-BH (central panel), and actin treated with CNBr after oxidation with 0.5 M t-BH (T, right panel). (B) Lyophilized actin was dissolved in 8 M urea and then treated overnight with t-BH at different concentrations. After exhaustive dialysis against buffer A for removing urea and the excess of t-BH, CNBr-induced fragmentation of oxidized actin was performed as described above. SDS−PAGE analysis of undigested actin (G, left panel), actin treated with CNBr after oxidation with different concentrations of t-BH in 8 M urea (central panel), and actin treated with CNBr after oxidation with 0.5 M t-BH in 8 M urea (T, right panel).

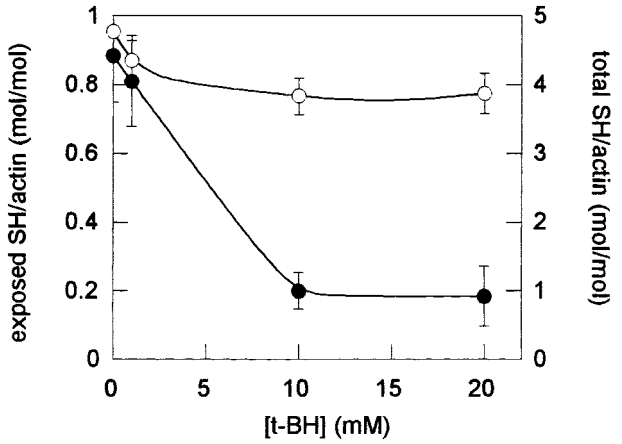

FIGURE 5: Effect of t-BH treatment on actin sulfhydryls. t-BH-treated G-actin solutions (11.82 μM), prepared as described in Figure 1, were added with DTNB, and the increase in absorbance caused by TNB anion release upon reaction of a thiol with DTNB was measured (filled circles). To unfold oxidized G-actin, thereby exposing and making reactive all actin sulfhydryl groups, actin monomers were lyophilized and then dissolved in 6 M GdmCl. After addition of DTNB, the absorbance of the TNB anion was measured (open circles). From the increased absorbance in protein samples caused by DTNB, the molar concentration of thiols present was calculated from the molar absorbance of the TNB anion. Error bars represent the standard deviations of three replicate measurements.

polymerization, during which the fluorescence intensity does not change. This is a steady state, with the amount of polymer determined by the rates of monomer addition to and loss from the ends of filaments (*38*). The steady-state fluorescence in actin samples oxidized with 1, 10, and 20 mM t-BH is about 5%, 14%, and 30% lower, respectively, than that of control. The lag prior to the fluorescence increase, i.e., the delay time, is due (at least in part) to actin nucleation, which is the formation of small actin oligomers acting as growing points for filament elongation. The delay time (t_d), calculated as suggested by Cooper et al. (*39*), is 1.34 min in control actin, and 1.34, 1.5, and 3.5 min in the actin samples oxidized with 1, 10, and 20 mM t-BH, respectively. The time ($t_{1/2}$) required for half-maximum assembly is about 4.4 min in control, and 4.4, 6.3, and 9.9 min in the actin samples oxidized with 1, 10, and 20 mM t-BH, respectively.

To characterize further the effect of oxidation produced by t-BH on the extent of actin polymerization, a high-speed sedimentation assay was used as an independent assay of polymerization. F-actin samples were centrifuged for 15 min at 350000*g*, and pellets were subjected to SDS−PAGE. The inhibitory effect of t-BH-induced actin oxidation on the final extent of polymerization is confirmed by the decrease in the amount of F-actin pelletable at high speed (not shown).

Critical concentration (C_c) values for oxidized F-actin were determined by measuring the steady-state values of high-shear viscosity (Figure 8). The C_c values (the intercept with the *x*-axis of the line connecting the specific viscosity values at various actin concentrations) for oxidized F-actin (C_c = 1.6, 3.0, and 3.6 μM for actin treated with 1, 10, and 20 mM t-BH, respectively) are higher than that for native F-actin (C_c = 1.35 μM). These data confirm that F-actin oxidized with t-BH reaches a final polymerization extent lower than that reached by native F-actin.

Effect of t-BH-Induced Oxidation on Actin Filament Elongation. To study the effect of oxidation produced by t-BH on actin filament elongation, we examined the nucleated polymerization of oxidized actin monomers. The lag phase at the onset of actin polymerization, initiated by the addition of neutral salt (spontaneous polymerization), is generally attributed to the actin nucleation reaction. However, when the nucleation is circumvented by adding phalloidin-stabilized nuclei ("seeds") with the polymerizing salt to initiate the polymerization, the increase in polymerization signal, at early times, is only due to the bidirectional growth of the added nuclei (elongation process). There is no lag phase, and the initial rate of polymer formation is linear with time and proportional to the elongation rate (*40*). Figure 9 shows the elongation of phalloidin-stabilized actin nuclei following addition of t-BH-treated actin monomers and polymerizing salts. Elongation of actin "seeds" occurring in the presence of oxidized actin monomers is considerably slower than that of control sample. The extent of inhibition of elongation rate depends on the t-BH concentration used to oxidize actin monomers. The maximum rate of fluores-

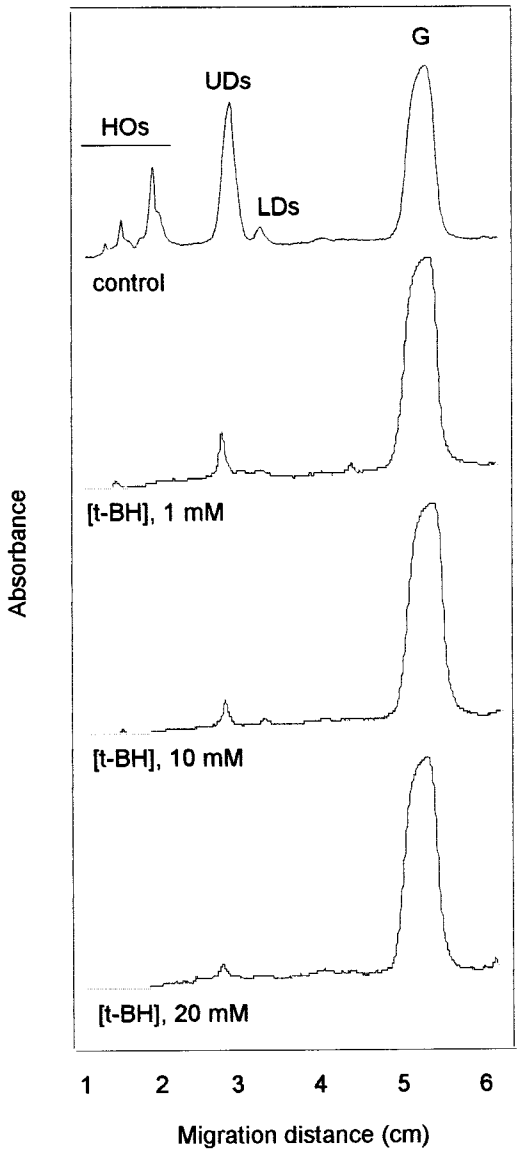

FIGURE 6: Intermolecular cross-linking between Cys-374 and Lys-191 in adjacent subunits of actin filaments. Oxidized G-actin solutions (11.82 μM), prepared as described in Figure 1, were incubated overnight in the presence of 100 mM KCl + 2 mM $MgCl_2$. Thereafter, aliquots were withdrawn and cross-linked with 1,4-PBM and then analyzed by SDS−PAGE on a 7.5% (w/v) gel. Densitometric scans of Coomassie blue-stained protein bands are shown. Positions of monomer (G), lower dimers (LDs), upper dimers (UDs), and higher molecular weight oligomers (HOs) are indicated.

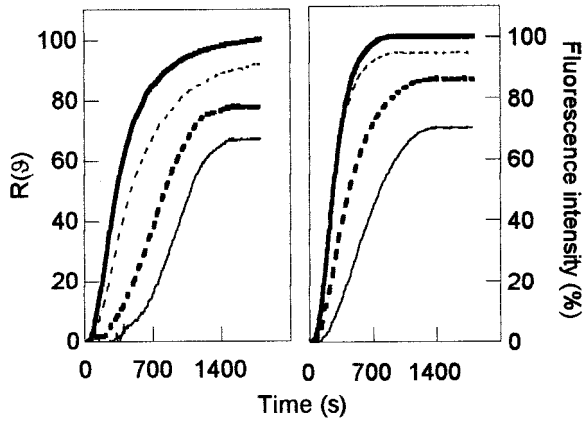

FIGURE 7: Time courses of actin polymerization. t-BH-treated G-actin solutions, prepared as described in Figure 1, were polymerized by the addition of 100 mM KCl + 2 mM $MgCl_2$. (Left panel) Light scattering intensity changes at 546 nm were followed continuously over the first 30 min time course. (Right panel) Fluorescence intensity changes were followed continuously over the first 30 min time course by the enhanced fluorescence of added pyrene-actin (5% of total actin). In both panels, native G-actin (thick solid trace), and G-actin treated with 1 mM (thin dashed trace), 10 mM (thick dashed trace), and 20 mM (thin solid trace) t-BH, respectively.

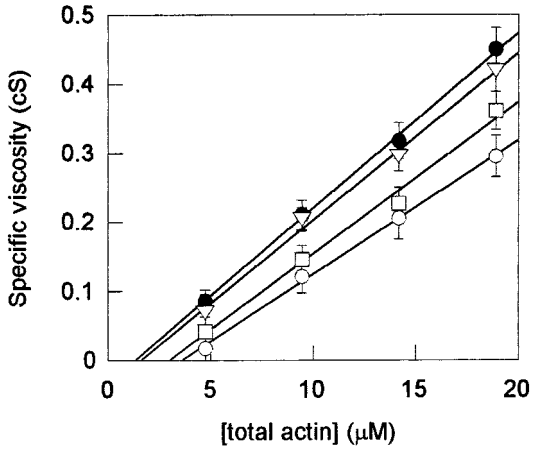

FIGURE 8: Determination of the critical concentration. Increasing concentrations (4.73−18.91 μM) of oxidized G-actin (prepared as described in Figure 1) were induced to polymerize by the addition of 100 mM KCl + 2 mM $MgCl_2$. The end points of specific viscosity were read after 18 h and plotted vs total actin concentration. Extrapolation of the line connecting the specific viscosity values at various actin concentrations to the *x*-axis yields the critical concentration. Native F-actin (filled circles), and F-actin assembled from monomers treated with 1 mM (open triangles), 10 mM (open squares), and 20 mM (open circles) t-BH, respectively. Error bars represent the standard deviations of three replicate measurements.

cence increase (elongation rate, determined from the initial rates of fluorescence change) is 0.7 IF s^{-1} in control, and 0.53, 0.29, and 0.18 IF s^{-1} in actin samples oxidized with 1, 10, and 20 mM t-BH, respectively.

DISCUSSION

The intrinsic tryptophan fluorescence of actin provides an effective and sensitive probe for measuring conformational changes occurring as a consequence of denaturation, exchange of the tightly bound Ca^{2+} for Mg^{2+}, or polymerization (*26*, *41*). In the present study, we have used the Trp intrinsic fluorescence as a probe for alterations in G-actin conformation induced by t-BH treatment. We observed a reduction of actin Trp fluorescence, without the spectral red shift characterizing denatured actin. The interpretation of the data is complicated by the presence of four Trp residues (Trp-79, Trp-86, Trp-340, and Trp-356) in rabbit muscle actin; therefore, intrinsic fluorescence changes are of uncertain origin. All four Trp residues of actin are confined to subdomain 1. Trp-79 and Trp-86 are in helix 74−92, the former partly exposed to the solvent and the latter fully exposed. Trp-340, in helix 338−348, and Trp-356, in loop 355−359, are completely buried, the latter being in a flexible region of the structure (*42*).

Tryptophan residues are among the preferred targets for the attack of oxidizing compounds, such as hydrogen peroxide and *N*-bromosuccinimide (NBS), resulting in the oxidation of the indole ring (e.g., see refs *43*−*46*). Therefore,

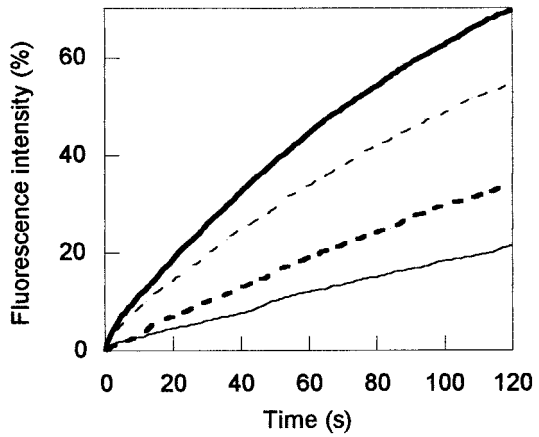

FIGURE 9: Elongation of phalloidin-stabilized actin nuclei ("seeds"). Elongation was started by the addition of 1350 μL of 11.82 μM oxidized G-actin (prepared as described in Figure 1 and added with 5% pyrene-actin) and 50 mM KCl + 1 mM $MgCl_2$ to 150 μL of actin seeds (2.45 μM). Native G-actin (thick solid trace), and G-actin treated with 1 mM (thin dashed trace), 10 mM (thick dashed trace), and 20 mM (thin solid trace) t-BH, respectively.

experiments were done to test for tryptophan oxidation by t-BH, although all the previous studies on this hydrophobic hydroperoxide reported that its amino acidic targets are cysteine and methionine residues (e.g., see refs *13*, *47*−*49*). Monitoring the possible loss of tryptophan by the change in the absorbance spectrum at 280 nm (*43*, *44*, *46*), we did not observe the characteristic UV absorption spectrum associated with Trp oxidation (not shown). As actin tryptophans are not oxidized by t-BH, the lowering of intrinsic fluorescence observed after t-BH treatment could reflect structural alterations in the G-actin molecule.

The observed structural changes induced by t-BH could be localized if we define the contribution of each of four Trp residues to intrinsic fluorescence. Given their location in different microenvironments (see above), the fluorescence spectra of the buried Trp-340 and Trp-356 residues must be blue, while those of the partially exposed Trp-79 and Trp-86 must be more red. In addition, quenching groups of tryptophan fluorescence are in close vicinity to Trp-79 and Trp-86 (*42*, *50*). Therefore, the quantum yield of these red spectrum tryptophan residues must be small. Hence, the fluorescence spectrum of G-actin must mainly be formed by the buried residues Trp-340 and Trp-356 (*51*). If Trp-340 and Trp-356 determine actin fluorescence, we can conclude that the t-BH treatment induces structural alterations in helix 338−348 and/or in loop 355−359 of the actin molecule.

Since fluorescence spectroscopy suggested that oxidation produced by t-BH results in changes in the correctly folded structure of monomeric actin, the conformational stability of oxidized actin has been determined. The study of protein unfolding by denaturation curves using urea is a convenient method for estimating the actin conformational stability. Under physiological conditions, the equilibrium of most proteins so greatly favors the native state that measuring the equilibrium constant for the folding/unfolding reaction is difficult. Titration of a protein solution with urea shifts the equilibrium between the native and denatured states of the protein to gradually favor the denatured form. Analysis of denaturation curves showed that oxidized actin unfolds at urea concentrations lower than that required for native actin denaturation and has a greater thermodynamic spontaneity to denature in the absence of denaturant, indicating that t-BH treatment has caused the monomers to become less stable.

As a valuable tool for probing local alterations in the tertiary structure of t-BH-treated actin monomers, we have used limited proteolysis by trypsin, α-chymotrypsin, and subtilisin. There are three regions in monomeric actin where its polypeptide chain can be enzymically cleaved by proteases with different specificity (*52*). These are surface loop 39−51, where α-chymotrypsin (*29*), subtilisin (*30*), and other enzymes cleave; segment 61−69 containing chymotryptic and tryptic cleavage sites (*53*); and the C-terminal segment which is accessible to numerous proteases (*52*). Oxidation of G-actin with t-BH did not influence the kinetics of actin decay during digestion with trypsin at Arg-62 and at Lys-68 (not shown). Differently, t-BH-induced oxidation renders the α-chymotrypsin cleavage site between Met-42 and Val-43 as well as the subtilisin cleavage site between Met-47 and Gly-48 less accessible, resulting in a decreased protease susceptibility of the surface loop 39−51 in subdomain 2 of the actin polypeptide chain. Thus, the structural perturbation of subdomain 2 by t-BH appears to be limited to loop 39−51.

Normal-mode analysis of the actin structure (*54*) predicts considerable movements of subdomains and individual loops in the molecule. Subdomain 2 of actin and its DNase-I-binding loop are the most mobile regions of the molecule (reviewed in ref *55*). Our observation that oxidation produced by t-BH renders loop 39−51 less susceptible to proteases suggests that in t-BH-treated G-actin this region assumes a more compact (less mobile) structure compared to native G-actin. One of the possibilities is that loop 39−51, extended and mobile in native G-actin, collapses onto the α-helix and β-sheet strands constituting the core of subdomain 2. Changes in the conformation of surface loop 39−51 induced by t-BH could influence actin polymerization in view of the involvement of the N-terminal portion of this loop (residues 40−45) in intermonomer interactions, as predicted by the atomic model of F-actin (*35*, *54*, *56*) and supported by evidence from biochemical studies (*57*, *58*). Our results on t-BH-oxidized actin polymerization support this evidence (see below).

At the t-BH concentrations used in this work, the CNBr cleavage pattern of oxidized G-actin appeared unaffected by the oxidative chemical treatment, indicating that oxidation of methionine residues did not occur. At much higher t-BH concentration (i.e., 0.5 M), the observed alteration in the CNBr cleavage pattern could result from the oxidation of exposed methionine residues, since t-BH appears to be capable of distinguishing between exposed methionine and buried methionine residues, being a specific oxidant for surface or exposed methionine residues (*13*).

Determination of both exposed and total thiols in G-actin indicated that the effect of different concentrations of t-BH is the oxidation of Cys-374, which is far more reactive than the other four Cys residues of the actin molecule (*33*).

Intermolecular cross-linking with 1,4-PBM, which covalently cross-links Cys-374, on one actin subunit, to Cys-374 (in the LD) or to Lys-191 (in the UD), on the adjacent subunit in the actin filament (*23*), showed that the quantity of LDs, UDs, and HOs decidedly decreased with the increase in t-BH concentration used to oxidize G-actin. This finding

could be due to either or both of two different mechanisms: oxidized G-actin could polymerize less than native actin, forming a lower amount of polymer; alternatively, oxidation of the SH group of Cys-374 renders it unsuitable for cross-linking by 1,4-PBM. Considering that the amounts of cross-linked dimers and oligomers in all the oxidized F-actin samples are less than 10% compared to control, while the quantity of oxidized F-actin sedimented in the high-speed centrifugation assay decreased by 30 and 41% compared to control in samples assembled from monomers oxidized with 10 and 20 mM t-BH, respectively, the second mechanism seems to be more plausible.

Many studies on derivatives of actin modified at Cys-374 showed that modification of this residue does not alter the rate or the extent of polymerization of actin (e.g., refs *19*, *39*, *59*−*62*). Alternatively, Tait and Frieden (*63*) showed that chemical modification of rabbit skeletal muscle actin at Cys-374 with *N*-ethylmaleimide (NEM) or with (iodoacetamido)-tetramethylrhodamine (IATR) accelerates the rate of polymerization and partially inhibits network formation. Moreover, *S*-(cysteine-374)glutathionyl actin polymerizes slowly and less efficiently compared to native actin and forms filaments that exhibit a diminished mechanical stability and an enhanced ATPase activity when exposed to shearing stress (*64*, *65*). On the other hand, Crosbie et al. (*66*) showed that both the pyrene and 1,5-IAEDANS probes attached to actin Cys-374, though not affecting actin polymerization, alter the structure of the nucleotide cleft, reducing its ability to exchange ATP and change, albeit differently from each other, the activation of myosin ATPase activity by actin and the in vitro motility of actin filaments. Moreover, using proteolytic digestion, they showed that the C-terminal region on actin is coupled to a distant DNase I site. The opposing effects of 1,5-IAEDANS and pyrene iodoacetamide on the ATPase activity and motility demonstrate that the nature of the probe determines the conformation of the C-terminus, and the resulting changes are transmitted throughout the molecule. However, these probe-dominated conformational changes at the actin's C-terminus were not defined. The local structure around Cys-374 in native actin is also uncertain given that the crystal structure of actin is lacking the last three C-terminal residues (*42*). It follows that different chemical modifications of the same, single amino acid residue can alter the properties of actin differently.

t-BH causes a marked slackening of the rate of actin polymerization. Polymerization of G-actin is commonly believed to involve at least three distinct steps: fast monomer activation, rate-limiting nucleation (both causing the initial lag phase), and moderately fast elongation (for reviews, see refs *67* and *68*). Nucleation can only be studied indirectly, because assays for dimers and trimers are not available. Thus, to understand whether the slower polymerization rate of oxidized actin was due to the slackening of nucleation and/or of the bidirectional growth of polymers, we monitored the elongation of preformed phalloidin-stabilized actin seeds so as to circumvent nucleation. The addition of oxidized actin monomers to the ends of phalloidin-stabilized actin seeds is very slow compared to that of native G-actin; this suggests that the decrease in the maximum polymerization rate is due (at least partly) to the slackening of oxidized monomer addition to growing ends of actin filaments. However, the involvement of an altered nucleation cannot be excluded. In addition, actin oxidation produced by t-BH alters the extent of polymerization, causing an increase (1.2−2.66-fold) in the steady-state monomer concentration and, consequently, a decrease in the final F-actin concentration.

At present, we can only speculate what in molecular terms caused the weakening of the interaction between the actin subunits. By oxidation with t-BH, an additional negative net charge is introduced into actin. This charge may increase the repellent forces between the anionic surfaces of the monomers that are thought to be neutralized by counterions when polymerization is started.

Both the oxidation of Cys-374 and the structural changes in surface loop 39−51 produced by t-BH could explain the slower and less efficient assembly of oxidized actin monomers. The structure of the C-terminal region, like that of the DNase-I-binding loop, is also highly mobile (*42*) and also has a role in the intermonomer interactions and in the integrity of F-actin; it has been shown that the chemical modification of Cys-374 with 2,4-dinitrophenylglutationyl disulfide (*65*, *69*) as well as removal of the last two or three C-terminal residues (*70*, *71*) destabilizes actin filaments. This destabilization appears to occur by a weakening of the interstrand connectivity generated by an allosteric conformational change in the actin filament (*72*). In addition, the existence of intermolecular coupling between loop 39−51 and the C-terminus in F-actin has been demonstrated (*73*). The C-terminus is conformationally coupled to other regions also within G-actin. Drummond et al. (*74*) as well as Crosbie et al. (*66*) demonstrated that structural changes at the C-terminus are transmitted to distant regions within the actin monomer and that these long-range communications may have functional significance. The structural alterations in surface loop 39−51 could be due to the allosteric intramonomer coupling between the DNase-I-binding loop and the C-terminal region of actin (the so-called "structural connectivity"). Studies with *Drosophila melanogaster* Act88F mutants containing altered C-terminal sequences showed that the substitutions and deletions in the C-terminus modulate not only the binding of ATP and profilin to actin, but also that of DNase I at a more distant part of actin (*74*). DNase I binding to the loop has been shown to introduce a new cleavage site at the distant C-terminus of G-actin (*66*). Moreover, in the atomic model of F-actin, the DNase-I-binding loop is involved in actin−actin contacts (*35*, *54*, *56*). More specifically, the DNase-I-binding loop of monomer *i* makes contact with loops 162−176 and 280−295 in subdomain 3 (*56*) or with residues in the cleft between subdomains 1 and 3 (*54*) of subunit *i*+2. This is consistent with the inhibition of actin polymerization by chemical modification of His-40 (*57*) and by proteolytic cleavage of the loop with subtilisin (*30*). Recently, Hegyi et al. (*75*) found that the *N*-(4-azido-2-nitrophenyl)putrescine (ANP) cross-links Gln-41 to Cys-374 on two adjacent actin monomers of the same strand in the long-pitch helix in F-actin. Therefore, given all of these various pieces of evidence, it is reasonable to expect that the formation of these intermonomer contacts is altered by structural changes directly or indirectly related to Cys-374 oxidation induced by t-BH.

REFERENCES

1. Stadtman, E. R. (1992) *Science 257*, 1220−1224.

2. Stadtman, E. R., and Oliver, C. N. (1991) *J. Biol. Chem. 266*, 2005−2008.
3. Bellomo, G., Jewell, S. A., Thor, H., and Orrenius, S. (1982) *Proc. Natl. Acad. Sci. U.S.A. 79*, 6842−6846.
4. Schraufstatter, I. U., Hinshaw, D. B., Hyslop, P. A., Spragg, R. G., and Cochrane, C. G. (1985) *J. Clin. Invest. 76*, 1131−1139.
5. Spragg, R. G., Hinshaw, D. B., Hyslop, P. A., Schraufstatter, I. U., and Cochrane, C. G. (1985) *J. Clin. Invest. 76*, 1471−1476.
6. Hinshaw, D. B., Sklar, L. A., Bohl, B., Schraufstatter, I. U., Hyslop, P. A., Rossi, M. W., Spragg, R. G., and Cochrane, C. G. (1986) *Am. J. Pathol. 123*, 454−464.
7. Hinshaw, D. B., Armstrong, B. C., Burger, J. M., Beals, T. F., and Hyslop, P. A. (1988) *Am. J. Pathol. 132*, 479−488.
8. Hinshaw, D. B., Burger, J. M., Beals, T. F., Armstrong, B. C., and Hyslop, P. A. (1991) *Arch. Biochem. Biophys. 288*, 311−316.
9. Mirabelli, F., Salis, A., Marinoni, V., Finardi, G., Bellomo, G., Thor, H., and Orrenius, S. (1988) *Arch. Biochem. Biophys. 264*, 261−269.
10. Omann, G. M., Harter, J. M., Burger, J. M., and Hinshaw, D. B. (1994) *Arch. Biochem. Biophys. 308*, 407−412.
11. DalleDonne, I., Milzani, A., and Colombo, R. (1995) *Biophys. J. 69*, 2710−2719.
12. Milzani, A., DalleDonne, I., and Colombo, R. (1997) *Arch. Biochem. Biophys. 339*(2), 267−274.
13. Keck, R. G. (1996) *Anal. Biochem. 236*(1), 56−62.
14. Caprari, P., Bozzi, A., Malorni, W., Bottini, A., Iosi, F., Santini, M. T., and Salvati, A. M. (1995) *Chem.-Biol. Interact. 94*, 243−258.
15. Lii, C.-H., and Hung, C.-N. (1997) *Biochim. Biophys. Acta 1336*, 147−156.
16. Spudich, J. A., and Watt, S. (1971) *J. Biol. Chem. 246*, 4866−4871.
17. Gordon, D. J., Yang, Y. Z., and Korn, E. D. (1976) *J. Biol. Chem. 251*, 7474−7479.
18. Tellam, R., and Frieden, C. (1982) *Biochemistry 21*, 3207−3214.
19. Kouyama, T., and Mihashi, K. (1981) *Eur. J. Biochem. 114*, 33−38.
20. Cooper, J. A., Walker, S. B., and Pollard, T. D. (1983) *J. Muscle Res. Cell Motil. 4*, 253−262.
21. Laemmli, U. K. (1970) *Nature 227*, 680−685.
22. Riddles, P. W., Blakeley, R. L., and Zerner, B. (1983) *Methods Enzymol. 91*, 49−60.
23. Millonig, R., Salvo, H., and Aebi, U. (1988) *J. Cell Biol. 106*, 785−796.
24. Stauffer, C. E., and Etson, D. (1969) *J. Biol. Chem. 244*, 5333−5338.
25. Cutruzzola, F., Ascenzi, P., Barra, D., Bolognesi, M., Menegatti, E., Sarti, P., Schnebli, H. P., Tomova, S., and Amiconi, G. (1993) *Biochim. Biophys. Acta 116*, 201−208.
26. Lehrer, S. S., and Kerwar, G. (1972) *Biochemistry 11*, 1211−1217.
27. Wegner, A., and Savko, P. (1982) *Biochemistry 21*, 1909−1913.
28. Estes, J. E., Selden, L. A., and Gershman, L. C. (1981) *Biochemistry 20*, 708−712.
29. Konno, K. (1987) *Biochemistry 26*, 3582−3589.
30. Schwyter, D., Philips, M., and Reisler, E. (1989) *Biochemistry 28*, 5889−5895.
31. Elzinga, M., Collins, J. H., Kuehl, W. M., and Adelstein, R. S. (1973) *Proc. Natl. Acad. Sci. U.S.A. 70*, 2687−2691.
32. Vandekerckhove, J., and Weber, K. (1978) *Eur. J. Biochem. 90*, 451−462.
33. Takashi, R. (1979) *Biochemistry 18*, 5164−5169.
34. Ellman, G. L. (1959) *Arch. Biochem. Biophys. 82*, 70−77.
35. Holmes, K. C., Popp, D., Gebhard, W., and Kabsch, W. (1990) *Nature 347*, 44−49.
36. Knight, P., and Offer, G. (1978) *Biochem. J. 175*, 1023−1032.
37. Elzinga, M., and Phelan, J. J. (1984) *Proc. Natl. Acad. Sci. U.S.A. 81*, 6599−6602.
38. Wegner, A. (1976) *J. Mol. Biol. 108*, 139−150.
39. Cooper, J. A., Loren Buhle, E., Walker, S. B., Tsong, T. Y., and Pollard, T. D. (1983) *Biochemistry 22*, 2193−2202.
40. Pollard, T. D. (1983) *Anal. Biochem. 134*, 406−412.
41. Selden, L. A., Kinosian, H. J., Estes, J. E., and Gershman, L. C. (1994) in *Actin: Biophysics, Biochemistry, and Cell Biology* (Estes, J. E., and Higgins, P. J., Eds.) pp 51−57, Plenum Press, New York.
42. Kabsch, W., Mannherz, H. G., Suck, D., Pai, E. F., and Holmes, K. C. (1990) *Nature 347*, 37−44.
43. Matsushima, A., Takiuchi, H., Saito, Y., and Inada, Y. (1980) *Biochim. Biophys. Acta 625*(2), 230−236.
44. Sanda, A., and Irie, M. (1980) *J. Biochem. 87*(4), 1079−1087.
45. Fox, T., Tsaprailis, G., and English, A. M. (1994) *Biochemistry 33*(1), 186−191.
46. Ray, S., Mukherji, S., and Bhaduri, A. (1995) *J. Biol. Chem. 270*(19), 11383−11390.
47. Van der Zee, J., Van Steveninck, J., Koster, J. F., and Dubbelman, T. M. (1989) *Biochim. Biophys. Acta 980*(2), 175−180.
48. Moore, R. B., Hulgan, T. M., Green, J. W., and Jenkins, L. D. (1992) *Blood 79*(5), 1334−1341.
49. Liu, J. L., Lu, K. V., Eris, T., Katta, V., Westcott, K. R., Narhi, L. O., and Lu, H. S. (1998) *Pharm. Res. 15*(4), 632−640.
50. McLaughlin, P. J., Gooch, J. T., Mannherz, H. C., and Weeds, A. G. (1993) *Nature 364*, 685−692.
51. Kuznetsova, I., Antropova, O., Turoverov, K., and Khaitlina, S. (1996) *FEBS Lett. 383*, 105−108.
52. Mornet, D., and Ue, K. (1984) *Proc. Natl. Acad. Sci. U.S.A. 81*, 3680−3684.
53. Jacobson, G. R., and Rosenbusch, J. P. (1976) *Proc. Natl. Acad. Sci. U.S.A. 73*, 2742−2746.
54. Tirion, M. M., ben-Avraham, D., Lorenz, M., and Holmes, K. C. (1995) *Biophys. J. 68*, 5−12.
55. Egelman, E. H., and Orlova, A. (1995) *Curr. Opin. Struct. Biol. 5*, 172−180.
56. Lorenz, M., Popp, D., and Holmes, K. C. (1993) *J. Mol. Biol. 234*, 826−836.
57. Hegyi, G., Premecz, G., Sain, B., and Muhlrad, A. (1974) *Eur. J. Biochem. 44*, 7−12.
58. Hegyi, G., Michel, H., Shabanowitz, J., Hunt, D. E., Chatterjie, N., Healy-Louie, G., and Elzinga, M. (1992) *Protein Sci. 1*, 132−144.
59. Lin, T.-I. (1978) *Arch. Biochem. Biophys. 185*, 285−299.
60. Ikkai, T., Wahl, P., and Auchet, J.-C. (1979) *Eur. J. Biochem. 93*, 397−408.
61. Wang, Y.-L., and Taylor, D. L. (1980) *J. Histochem. Cytochem. 28*, 1198−1206.
62. Taylor, D. L., Reidler, J. A., Spudich, J. A., and Stryer, L. (1981) *J. Cell Biol. 89*, 362−367.
63. Tait, J. F., and Frieden, C. (1982) *Biochemistry 21*, 6046−6053.
64. Faulstich, H., Merkler, I., Blackholm, H., and Stournaras, C. (1984) *Biochemistry 23*, 1608−1612.
65. Stournaras, C., Drewes, G., Blackholm, H., Merkler, I., and Faulstich, H. (1990) *Biochim. Biophys. Acta 1037*, 86−91.
66. Crosbie, R. H., Miller, C., Cheung, P., Goodnight, T., Muhlrad, A., and Reisler, E. (1994) *Biophys. J. 67*, 1957−1964.
67. Pollard, T. D. (1990) *Curr. Opin. Cell Biol. 2*, 33−40.
68. Estes, J. E., Selden, L. A., Kinosian, H. J., and Gershman, L. C. (1992) *J. Muscle Res. Cell Motil. 13*, 272−284.
69. Drewes, G., and Faulstich, H. (1990) *J. Biol. Chem. 265*, 3017−3021.
70. O'Donoghue, S. I., Miki, M., and dos Remedios, C. G. (1992) *Arch. Biochem. Biophys. 293*, 110−116.
71. Mossakowska, M., Moraczewska, J., Khaitlina, S., and Strzelecka-Golaszewska, H. (1993) *Biochem. J. 289*, 897−902.
72. Orlova, A., Prochniewicz, E., and Egelman, E. H. (1995) *J. Mol. Biol. 245*, 598−607.
73. Kim, E., and Reisler, E. (1996) *Biophys. J. 71*, 1914−1919.
74. Drummond, D. R., Hennessey, E. S., and Sparrow, J. C. (1992) *Eur. J. Biochem. 209*, 171−179.
75. Hegyi, G., Mák, M., Kim, E., Elzinga, M., Muhlrad, A., and Reisler, E. (1998) *Biochemistry 37*, 17784−17792.

BI990367K